PROCEEDINGS OF SPIE

SPIEDigitalLibrary.org/conference-proceedings-of-spie

R4AsH: a triple frequency laboratory radar for characterizing falling volcanic ash

Macfarlane, David, Robertson, Ducan, Capponi, Antonio

David G. Macfarlane, Ducan A. Robertson, Antonio Capponi, "R4AsH: a triple frequency laboratory radar for characterizing falling volcanic ash," Proc. SPIE 11742, Radar Sensor Technology XXV, 1174219 (12 April 2021); doi: 10.1117/12.2587613

SPIE.

Event: SPIE Defense + Commercial Sensing, 2021, Online Only

Downloaded From: https://www.spiedigitallibrary.org/conference-proceedings-of-spie on 22 Apr 2021 Terms of Use: https://www.spiedigitallibrary.org/terms-of-use

R4AsH: a triple frequency laboratory radar for characterizing falling volcanic ash

David G. Macfarlane *[a], Duncan A. Robertson[a], Antonio Capponi[b]
[a]University of St Andrews, SUPA School of Physics & Astronomy, St Andrews, Fife KY16 9SS, UK; [b]Lancaster Environment Centre, LEC Building, Lancaster, Lancashire LA1 4YQ, UK

ABSTRACT

Airborne ash generated by explosive volcanic eruptions presents a significant danger to aviation. Accurate modelling and predictions of the dispersal of hazardous ash into the atmosphere are currently hampered by uncertainties in the 'source term' parameters associated with the initial eruption plume, specifically the amount and size of ash particles released into the atmosphere. Ground based radar offers the means to remotely measure ash reflectivity, however estimation of source term parameters from reflectivity measured by single frequency radar is limited by ambiguity between the contribution of particle size distribution (PSD) and ash concentration in the plume. This means that one of these parameters must be assumed rather than measured directly, leading to uncertainties in forecasting eruption hazards. We report on R4AsH, a close range FMCW radar designed to resolve this ambiguity by simultaneous characterization of falling volcanic ash in a laboratory-controlled environment at three different frequencies: 10, 35 and 94 GHz. The R4AsH design uses a single DDS based chirp generator as a common source, multiplied and upconverted to feed three sets of transmit-receive horn antennas directed at a common target volume such that measurements will give spatially and temporally coincident measurements of falling ash. In addition, there will be independent measurement of the PSD using optical imaging and logging of the landing particle mass to calibrate results and inform analysis. The aim of R4AsH is to develop a triple-frequency inversion algorithm to enable simultaneous retrieval of PSD and ash concentration from radar data suitable for future volcano monitoring systems.

Keywords: Volcanic Ash, FMCW radar, Radar Cross Section, Reflectivity, Horn antenna, Multi-frequency

1. INTRODUCTION

1.1 Background

The 2010 eruption of the Eyjafjallajökull volcano in Iceland affected air traffic across Europe between the 15th and 23rd April with the associated closure of European airspace stranding 10 million passengers and costing the airline industry approximately USD1.7 billion[1]. The risks to aviation are significant and aircraft encounters with ash can produce effects ranging from a loss in air quality within the aircraft through instrumentation damage from blockage or abrasion up to the most serious event of engine failure caused by ash melting and fusing to components within jet engines[2]. Avoiding the dangers and alleviating costs of volcanic eruptions to aviation could be achieved by improving our ability to predict the precise location of hazardous airborne ash, however this is currently limited by the uncertainties involved in gathering timely observational data on eruptions as they evolve. Sampling of ash via instrumented aircraft has been used to inform and develop sophisticated models of ash transport and dispersion in the atmospehere[3] but the uncertainties remain such that advisories by aviation authorities have to err on the side of caution and close larger areas of airspace than is strictly necessary. Ground based radar observation of ash could help by providing temporally and spatially significant improvements in monitoring the output of volcanoes but the most common radar systems, which operate at microwave frequencies, are designed for meteorological observations and are not optimized for measuring volcanic ash[4]. One of the largest uncertainties remains in the monitoring of volcanic eruption columns. For most eruptions there is simply a lack of knowledge of the 'source-term', i.e. details of the height, size, distribution and density of ash being erupted which would be invaluable for predicting dispersion of ash into the atmosphere. The R4AsH project[5] is a new collaboration designed to improve our understanding of the radar signatures of volcanic ash via laboratory investigation into the backscatter of falling volcanic ash at multiple frequencies. The end goal of the project is to develop a new inversion algorithm that can be used to inform the design of ground based radar systems that could remotely measure ash particle sizes and densities at or near volcanic eruptions to provide timely data for forecasting the location of ash hazardous to aviation.

*dgm5@st-andrews.ac.uk.; phone +44 1334 461608;

Radar Sensor Technology XXV, edited by Kenneth I. Ranney, Ann M. Raynal, Proc. of SPIE Vol. 11742
1174219 · © 2021 SPIE · CCC code: 0277-786X/21/$21 · doi: 10.1117/12.2587613

Downloaded From: https://www.spiedigitallibrary.org/conference-proceedings-of-spie on 22 Apr 2021
Terms of Use: https://www.spiedigitallibrary.org/terms-of-use

2. R4ASH DESIGN

2.1 R4AsH experimental concept

The basic concept of the R4AsH experiment is to characterize the backscatter properties of volcanic ash by simultaneously measuring a volume of falling ash at three different radar frequencies as well as using optical methods to capture the particle size distribution (PSD) within the volume (Fig 1.). The optically sampled PSD will then be used as the basis to develop radar inversion algorithms and confirm the PSD as inferred by analysis of the triple frequency radar backscatter data. The target particles will be contained within a reservoir at the top of the experiment with mechanical release and sieving mechanisms to allow control of particle size and flow rates of ash into the sampling volume below. We chose three frequencies to examine the ash: 10 GHz as it is a commonly used frequency in weather radar, 35 GHz and 94 GHz as they are two well separated frequencies that span the transition from Rayleigh to Mie scattering for ash particles of the size of interest. The aim is to investigate the statistical differences in radar response to ash as a function of frequency and determine the most significant signatures relating to determination of the ash PSD.

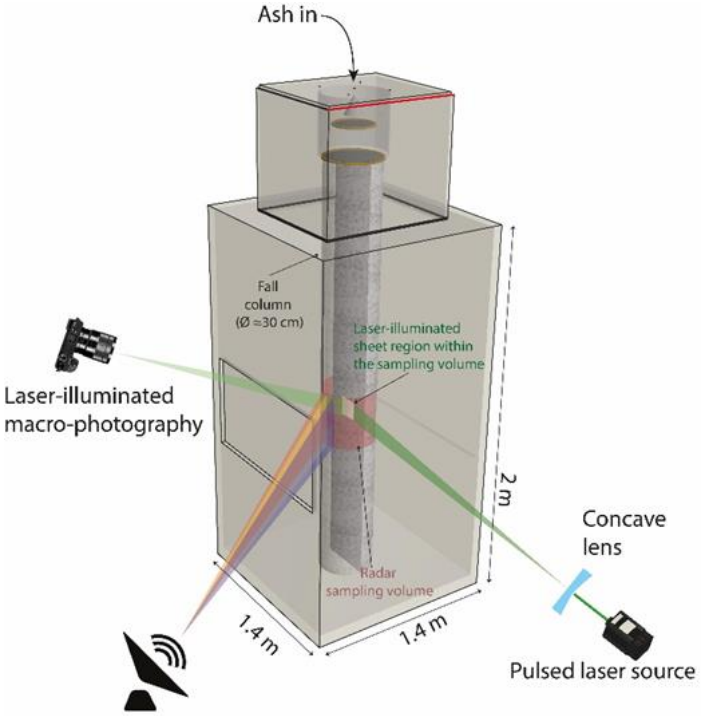

Figure 1. R4AsH experiment concept: a controlled fall of volcanic ash is simultaneously sampled by three radar frequencies and flash illuminated photography to measure the radar signatures and particle size distribution of the falling ash

2.2 Design Choices

The R4AsH design is a low power Frequency Modulated Continuous Wave (FMCW) radar that avoids the limitations of operating at very short range using pulsed techniques. The first fundamental design constraint put on the R4AsH experiment was deciding upon a practical volume size for which an ash fall could be maintained for tens of seconds in a controlled laboratory environment. We decided that a column of 300 mm diameter would be achievable and a radar range resolution of 150 mm, and hence chirp bandwidth of 1 GHz, would be required to ensure the sampling bin is entirely within the column. Similarly, we constrained the radar beam width to have dimensions within this column of ash. The antennas are 24.5 dBi gain smooth-walled feedhorns which have a triple-linear profile based on Granet's design[6]. Such horns have previously been designed and manufactured in St Andrews at 24 and 94 GHz with performance showing excellent agreement with theory[7] produced using CORRUG mode matching software[8]. The profile of these horns can be scaled directly with wavelength and offered a reliable and predictable set of antenna patterns for in-house manufacture at the new frequencies of 10 and 35 GHz. The physical lengths of the horns are 700 mm at 10 GHz, 226 mm at 35 GHz and 77 mm at 94 GHz. These horn antennas have been manufactured in house in St Andrews and their antenna patterns measured showing excellent agreement with theory (Figure 2.)

Downloaded From: https://www.spiedigitallibrary.org/conference-proceedings-of-spie on 22 Apr 2021
Terms of Use: https://www.spiedigitallibrary.org/terms-of-use

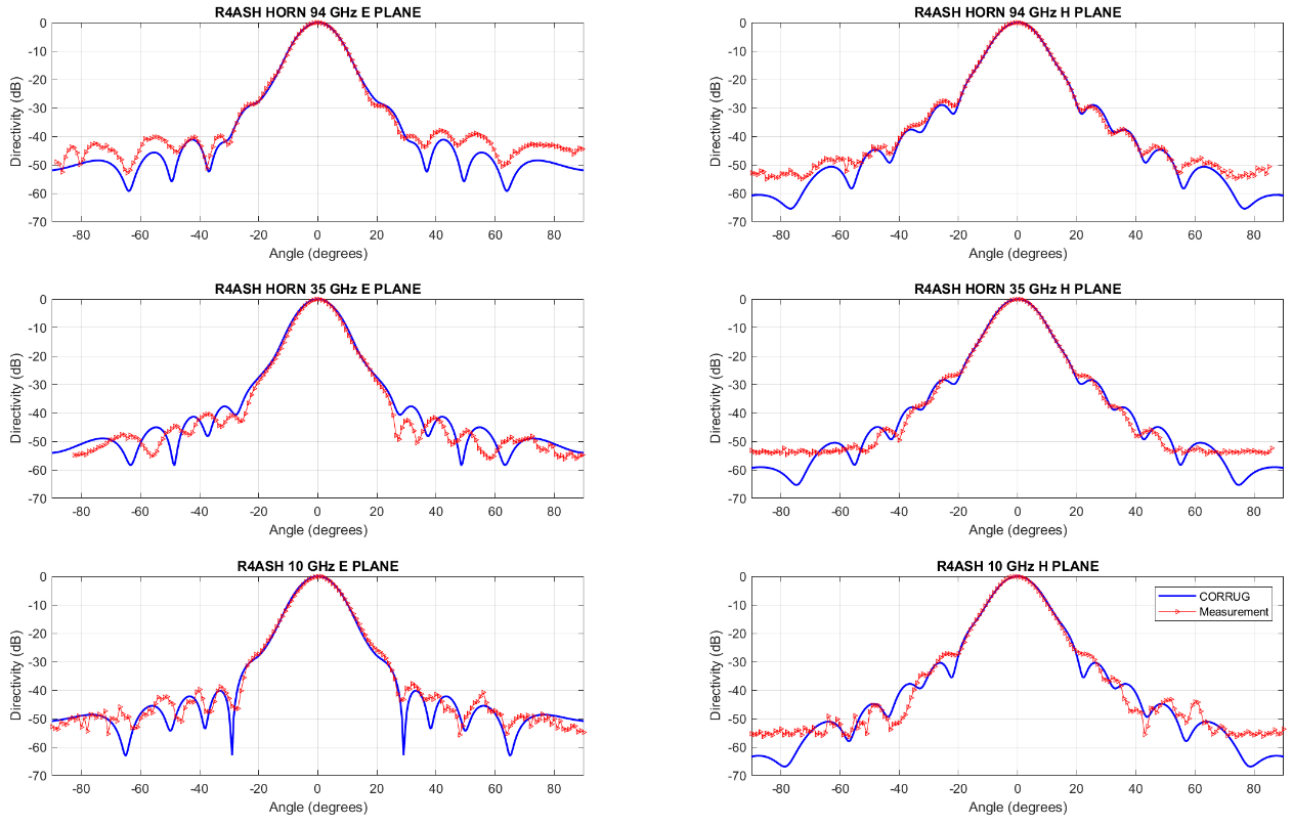

Figure 2. R4AsH Horn Antenna Patterns. E and H plane measurements shown for one horn at each frequency alongside CORRUG predicted patterns.

The horns have a 11.4° 3dB beam angle in both principal planes, so assuming a 300 mm ash column diameter constrained the experiment to use a particularly short radar operating distance of approximately 1meter at which the lateral beam width is ~200 mm.

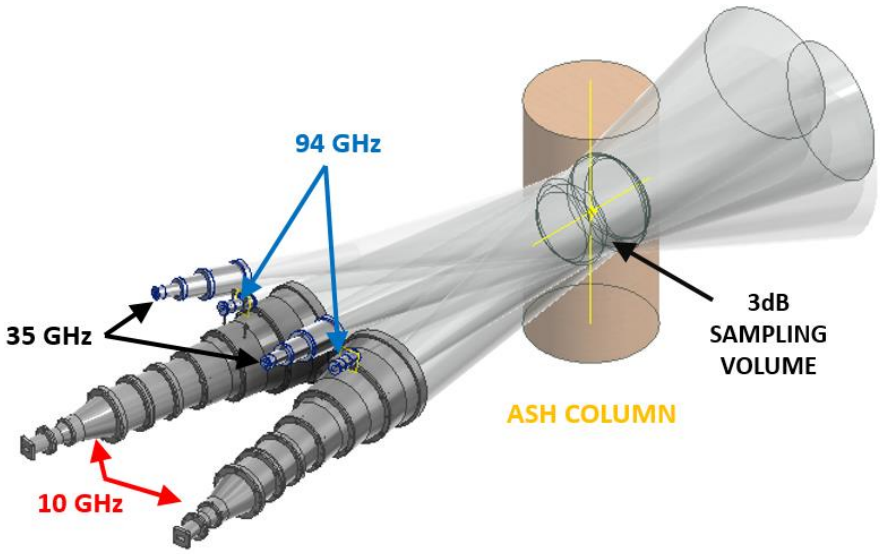

Figure 3. 3D CAD scale diagram of the R4AsH antenna beam layout. The three pairs of horns have optical axes passing through the centre of the ash column at a range of 1 m from the phase centre of each horn.

Downloaded From: https://www.spiedigitallibrary.org/conference-proceedings-of-spie on 22 Apr 2021
Terms of Use: https://www.spiedigitallibrary.org/terms-of-use

To assess the practical placement of the horns, CAD models of each horn were constructed in Autodesk Inventor with the beam represented as a 11.4° cone fixed to the phase centre of each horn (Fig. 3). Near field beams limits were crudely approximated in CAD using cylinders of equal diameter to each horn aperture to show possible beam occlusions. The horns positions were then parameterized to rotate around the centre of the ash column so that physical horn placement could be finalized. For the beams to cross at the centre of the ash column the 10 GHz horns were mounted on the same elevation plane but limited to an azimuthal bistatic angle of 18° to avoid the front of the horns physically clashing. The large size of the 10 GHz horns then limited the elevation positions of the 35 and 94 GHz horn pairs to a look down angle of 11°. Their azimuthal bistatic angles were then chosen to also be 18° (with a 6° offset between pairs) to maintain similarity with the 10 GHz optics. With the optics chosen, the next step was to constrain the experiment ash parameters and then calculate radar reflectivity of the sampling volume and thus power reflected to the radar.

2.3 RF Design Overview

The RF design for R4AsH is based on FMCW radar architectures previously developed in St Andrews[9] and employs a common DDS chirp generator split into three channels for upconversion to the radar bands of interest. A simplified block diagram of the system is given below (Fig.4).

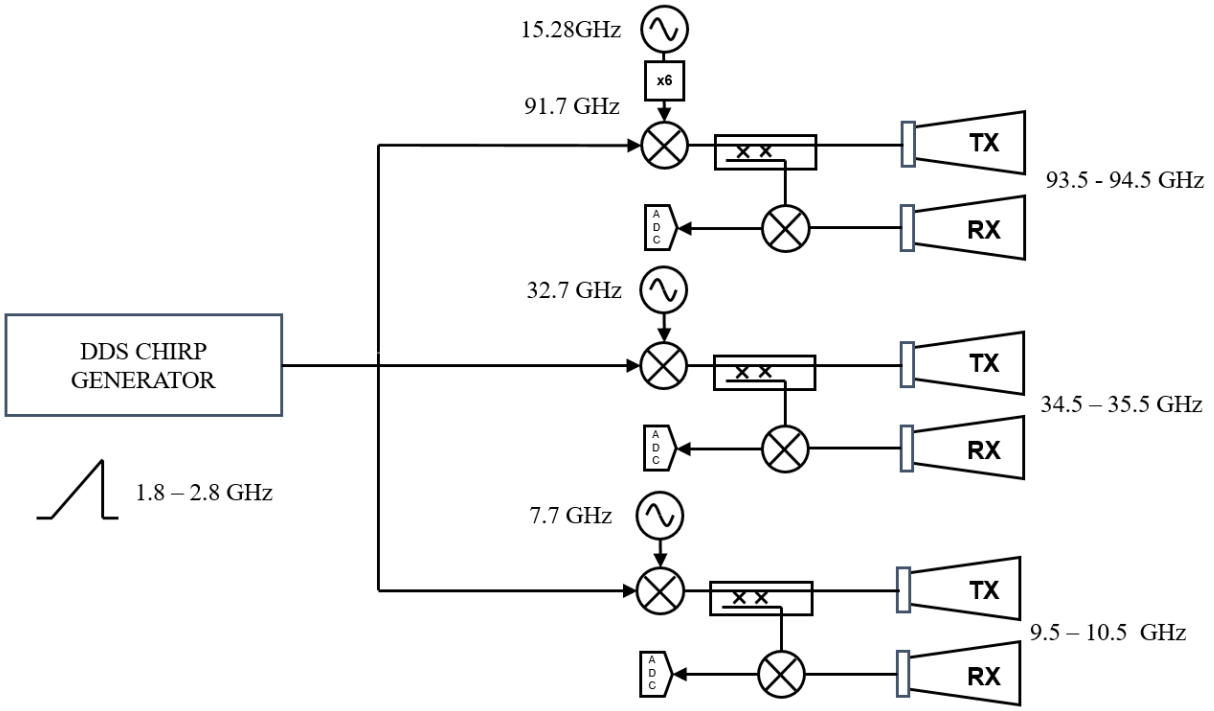

Figure 4. Simplified R4AsH RF block diagram. A common DDS based chirp generator is split three ways and upconverted to provide identical bandwidth chirps at the three chosen centre frequencies of 10, 35 and 94 GHz. Receive channels are sampled simultaneously by a common ADC

Since the prime aim is to have simultaneous sampling of the ash volume at each radar frequency a single chirp generator is upconverted onto each radar channel. Thus each channel has the same bandwidth so that the range resolution is identical for each channel. To achieve fast chirps (32 μs) with high linearity and low phase noise, we use a customized Analog Devices AD9914 direct digital synthesis (DDS) evaluation board clocked at 3.5 GHz. The range resolution requirement of 150 mm translates to a bandwidth of 1 GHz which is achieved by sweeping the DDS from 0.9 to 1.4 GHz and then doubling to 1.8 to 2.8 GHz. This signal is filtered, amplified and then split three ways to give appropriate power levels to allow upconversion against three separate free running dielectric resonator oscillators (FRDROs) at 7.7, 32.7 and 15.28 GHz multiplied by 6 to give 91.7 GHz. Following further bandpass filtering to suppress unwanted mixer products, each channel is then amplified at the carrier bandwidth such that there is enough power to drive the LO of its receiving mixer via directional couplers. Amplification levels were also chosen to provide enough transmit power for sufficient signal to noise returned by the ash in the receiving channels. The level of amplification was chosen after analysis of the expected power returns from the ash column as described in the following section.

Downloaded From: https://www.spiedigitallibrary.org/conference-proceedings-of-spie on 22 Apr 2021
Terms of Use: https://www.spiedigitallibrary.org/terms-of-use

2.4 Power budget

In meteorological radar systems, volume scattering is commonly modelled using the Probert-Jones approximation[10] which assumes a Gaussian profile in power across the radar beam. Here we recast the original equation which described a pulsed radar system for a close-range FMCW analysis. The well-known radar range equation for power received by a radar from a point target is

$$P_r = \frac{P_t G^2 \lambda^2}{(4\pi)^3 R^4} \sigma \tag{1}$$

where P_t is the power transmitted, G the antenna gain (here the same for transmit and receive), λ the radar wavelength, R the range to target and σ is the Radar Cross Section (RCS) of the target. For volumetric targets, σ is the product of the radar reflectivity (per unit volume), η, and the volume itself:

$$\sigma = \eta V \tag{2}$$

For a pencil beam, the Probert-Jones approximation for the volume of a range cell is

$$V = \frac{\pi \theta \phi R^2 \Delta R}{4} \tag{3}$$

This is a far-field approximation of a truncated cone, assuming that the azimuth one-way 3dB beamwidth θ and the elevation one-way 3dB beamwidth ϕ are small angles at a large distance[11], i.e. the one-way beam diameters are approximated by $R\theta$ and $R\phi$. Thus, the beam radii are $R\theta/2$ and $R\phi/2$ and the area of the circle at each end of the truncated cone is approximately

$$A = \pi \cdot \frac{\theta R}{2} \cdot \frac{\phi R}{2} = \frac{\pi \theta \phi R^2}{4} \tag{4}$$

Thus with an FMCW range resolution of $\Delta R = c/2B$ the volume of the sampling cell will be approximated by

$$V = \frac{\pi \theta \phi R^2}{4} \cdot \frac{c}{2B} \tag{5}$$

Following the Probert-Jones analysis there is also a factor of 2ln2 to account for the Gaussian profile of the beam, i.e.

$$V = \frac{\pi \theta \phi R^2}{2 \ln 2 \cdot 4} \cdot \frac{c}{2B} \tag{6}$$

Thus for an FMCW radar the radar equation for a volumetric target is

$$P_r = \frac{P_t G^2 \lambda^2}{(4\pi)^3 R^4} \cdot \frac{\pi \theta \phi R^2}{8 \ln 2} \cdot \frac{c}{2B} \cdot \eta \tag{7}$$

Here the radar equation has been parsed into four terms. The first is essentially a radar system term, the second the area of beam intercepting the scattering volume and the third the range resolution (and hence radial extent) of the sampling volume. The second and third terms are of particular interest as the optics for the 10 GHz antennas will not be in the far field approximation due to the short target range of 1 m. The intention is to measure the actual beam volume to account for the widening of the beam in the near field.

The fourth term for reflectivity, η, is the only term that is not system dependent. Estimation of η was critical to the system design as it informs the power budget for each channel. Reflectivity can be calculated by summing the RCS values for ash particles of a given diameter across an assumed distribution of particle sizes, i.e.

$$\eta = \int_{D_{min}}^{D_{max}} \sigma(D) N(D) dD \tag{8}$$

where $\sigma(D)$ is the backscatter RCS of particles with diameter D and $N(D)dD$ is the number of particles having diameters between D and $D+dD$ per unit volume, i.e. the ash PSD.

The next step was to model a realistic PSD and constrain the range of particle sizes under consideration. Previous work by Marzano et al[12] provided us with a set of nine different ash categories as a combination of three different concentrations and three different diameters (Table 1).

Downloaded From: https://www.spiedigitallibrary.org/conference-proceedings-of-spie on 22 Apr 2021
Terms of Use: https://www.spiedigitallibrary.org/terms-of-use

Table 1. Ash categories

The Marzano Ash Categories			
Concentrations		Mean Diameters	
Light:	0.1 g/m^3	Fine:	0.01 mm
Moderate:	1 g/m^3	Coarse:	0.1 mm
Intense:	5 g/m^3	Lapilli:	1 mm

With particle size as large as 1 mm (which is comparable in size to the 94 GHz wavelength of 3.2 mm) one cannot use Rayleigh scattering to model RCS here and instead particle RCS values were calculated using the Mie scattering formula:

$$\sigma(D) = \frac{\lambda^2}{4\pi} \left|\sum_{n=1}^{\infty}(-1)^n(2n+1)(a_n - b_n)\right|^2 \quad (8)$$

where n is a positive integer and the a_n and b_n are Mie coefficients which in turn depend upon the size and dielectric properties of the target material. We assumed a complex permittivity for ash of 6.15 - 0.15j taken from the average results of the W-band measurements on dry compacted ash samples by Rogers et al[13]. A more detailed description of Mie coefficients can be found elsewhere in the literature[14]. Here for the ash PSD, we replicated and confirmed modelling work on volcanic ash reflectivity from 1 GHz to 1 THz by Speirs[15] (following Marzano) who used a normalised gamma distribution:

$$N(D) = \frac{6C_a D_n^{\mu}}{\pi\rho_{ash}(3+\mu)!}\left(\frac{(\mu+1)!}{D_n(\mu!)}\right)^{4+\mu}\left(\frac{D}{D_n}\right)^{\mu}\exp\left(-(\mu+1)\frac{D}{D_n}\right) \quad (9)$$

where C_a is the ash concentration (gm^{-3}), D_n is the mean particle diameter (m), ρ_{ash} is the solid density of ash (1x 10^6 gm^{-3}) and μ is a shape parameter chosen here to equal 1 (which both Speirs and Marzano used for a normalized gamma distribution).

The calculations of η of are plotted below (Fig. 5) with the R4AsH category numerical values tabulated in Table 2.

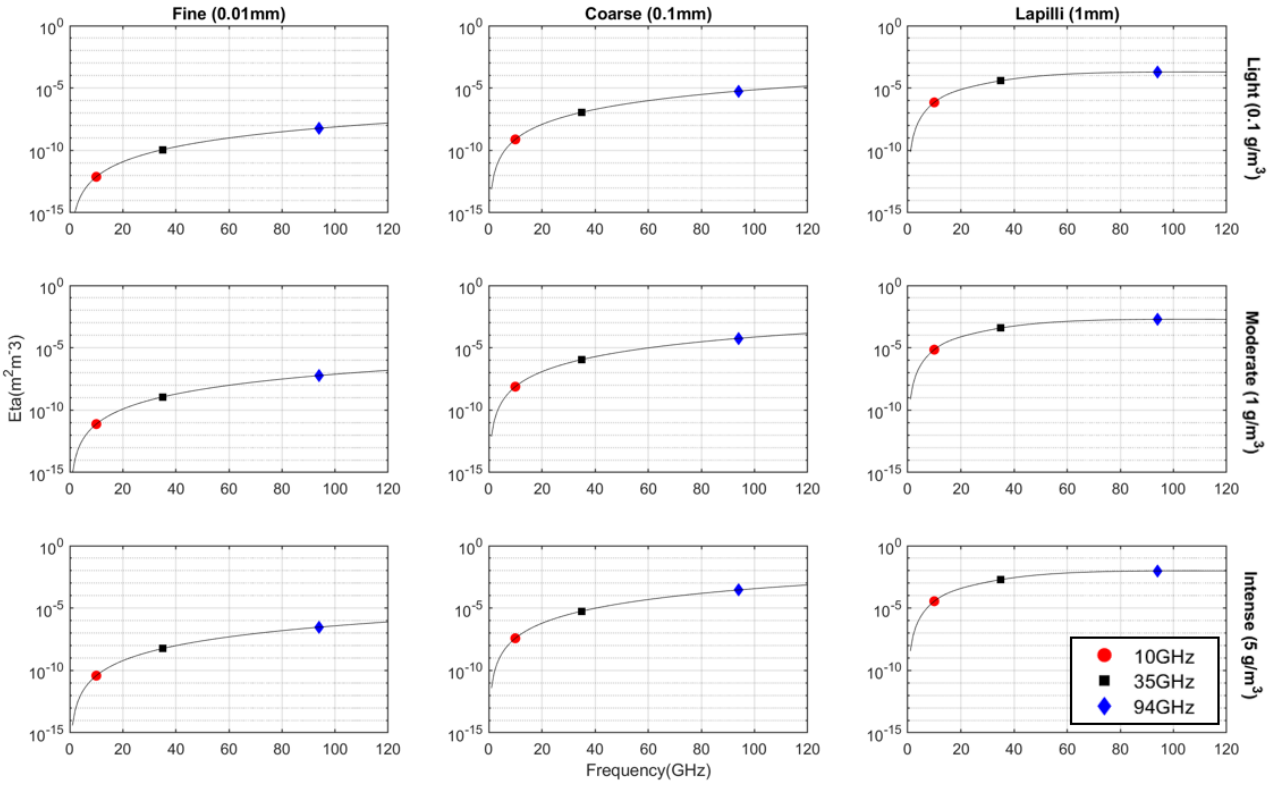

Figure 5. Reflectivity of volcanic ash for the nine Marzano categories with R4AsH carrier frequencies indicated.

Downloaded From: https://www.spiedigitallibrary.org/conference-proceedings-of-spie on 22 Apr 2021
Terms of Use: https://www.spiedigitallibrary.org/terms-of-use

Table 2. Reflectivity values for R4AsH channels corresponding to graphs shown in Figure 5.

Marzano Ash Categories		**Eta (m^2m^{-3})**			**10 log 10(Eta) (dB)**		
Diameter (mm)	Concentration (g/m^3)	10 GHz	35 GHz	94 GHz	10 GHz	35 GHz	94 GHz
0.01	0.1	7.588E-13	1.139E-10	5.923E-09	-121.20	-99.44	-82.27
0.10	0.1	7.586E-10	1.135E-07	5.713E-06	-91.20	-69.45	-52.43
1.00	0.1	7.093E-07	3.840E-05	1.933E-04	-61.49	-44.16	-37.14
0.01	1	7.588E-12	1.139E-09	5.923E-08	-111.20	-89.44	-72.27
0.10	1	7.586E-09	1.135E-06	5.713E-05	-81.20	-59.45	-42.43
1.00	1	7.093E-06	3.840E-04	1.933E-03	-51.49	-34.16	-27.14
0.01	5	3.794E-11	5.693E-09	2.962E-07	-104.21	-82.45	-65.28
0.10	5	3.793E-08	5.677E-06	2.856E-04	-74.21	-52.46	-35.44
1.00	5	3.546E-05	1.920E-03	9.666E-03	-44.50	-27.17	-20.15

The range in reflectivity across the R4AsH bands is very large (~100 dB). Even within each R4AsH band there is a large range between minimum and maximum levels of reflectivity: 76.7 dB at 10 GHz, 72.3 dB at 35 GHz and 62.1 dB at 94 GHz. Using equation (2) one can calculate the RCS for each category with the 3 dB sampling volume occupying 3.35 x 10^{-3} m^3. As RCS drops by around 20 dB between each channel, transmit power was increased to compensate for the drop in reflectivity as the frequency reduces. The minimum and maximum powers received were then calculated using equation (7) with R = 1 m, G = 24.5 dB, B = 1 GHz and λ as appropriate for the centre of each channel and P_t as given in Table 3.

In addition, consideration was given to the clutter backscatter levels for the experimental chamber. The back wall of the chamber will be lined with Wavasorb VHP-4 from Emerson and Cuming[16] at a slightly more distant range of 1.5 m. This absorber presents a beam filling RCS of at -60 dBsm or better across the R4AsH bands allowing us to calculate the maximum expected clutter returns from the experimental setup. The aim was to have clutter levels at a similar level to the maximum ash returns so that the receiving channels would not be saturated by clutter returns. Note that although $\sigma_{clutter}$ has a similar RCS to the expected σ_{max} values, the clutter lies at a different range to the ash returns and will be range gated out in the experiment.

Table 3. RCS values, Power received and Signal to Noise ratios for the R4AsH channels

	10 GHz	**35 GHz**	**94GHz**
σ_{min} (dBsm)	-146.0	-124.2	-107.0
σ_{max} (dBsm)	-69.3	-51.9	-44.9
$\sigma_{clutter}$ (dBsm)	-60.0	-60.0	-60.0
P_t (dBm)	32.2	25.9	19.9
P_r min (dBm)	-128.2	-123.6	-121.0
P_r max (dBm)	-51.5	-51.3	-58.9

Downloaded From: https://www.spiedigitallibrary.org/conference-proceedings-of-spie on 22 Apr 2021
Terms of Use: https://www.spiedigitallibrary.org/terms-of-use

3. CONCLUSIONS AND FUTURE WORK

We have presented an outline of the R4AsH experiment to investigate the radar properties of airborne volcanic ash and the design calculations used to determine the expected reflectivity of volcanic ash at 10, 35 and 94GHz. The R4AsH experiment is scheduled to take place in the summer of 2021 and we expect to start development of the experimental procedure and radar inversion algorithm techniques in the near future. We also wish to thank Mr. Aleksanteri Vattulainen for his assistance in measuring the far field antenna patterns of the R4AsH horns.

REFERENCES

[1] Mazzocchi M., Francesca Hansstein, F. and Ragona, M., "The 2010 Volcanic Ash Cloud and Its Financial Impact on the European Airline Industry," CESifo Forum, ifo Institute - Leibniz Institute for Economic Research at the University of Munich, vol. 11(02), 92-100 (2010)

[2] Alexander, D. "Volcanic ash in the atmosphere and risks for civil aviation: A study in European crisis management" Int J Disaster Risk Sci 4, 9–19 (2013). https://doi.org/10.1007/s13753-013-0003-0

[3] Dacre, H. F., Grant, A. L. M., and Johnson, B. T. "Aircraft observations and model simulations of concentration and particle size distribution in the Eyjafjallajökull volcanic ash cloud", Atmos. Chem. Phys., 13, 1277–1291 (2013) https://doi.org/10.5194/acp-13-1277-2013, 2013.

[4] Marzano, F.S., Picciotti E., Montopoli, M. and Vulpiani G., "Inside volcanic clouds — remote sensing of ash plumes using microwave weather radars", Bull. Am. Meteorol. Soc., 94, 1567-1586, (2013) 10.1175/BAMS-D-11-00160.1

[5] http://wp.lancs.ac.uk/radar-forecasting-of-volcanic-ash/ (17 March 2021).

[6] Granet C., Bolton R. and Moorey G., "A smooth-walled spline-profile horn as an alternative to the corrugated horn for wide band millimeter-wave applications, " IEEE Trans. Antennas Propag., 52 (3), 848–854 (2004)

[7] Rahman, S. and Robertson, D.A., "Coherent 24 GHz FMCW radar system for micro-Doppler studies", Proc SPIE 10633, Radar Sensor Technology XXII; 106330I (2018) https://doi.org/10.1117/12.2304368

[8] "CORRUG, SMT Consultancies Ltd Home", http://www.smtconsultancies.co.uk/products/corrug/corrug.php (17 March 2021).

[9] Robertson, D.A., "Enabling Technologies for High Performance Millimetre and Sub-millimetre Wave Radar", Proc. International Radar Symposium, 1 – 10, (2018) https://doi.org/10.23919/IRS.2018.8448180

[10] Probert-Jones, J.R., "The radar equation in meteorology", Quart. J. Roy. Meteor. Soc., 88, 485–495 (1962)

[11] Currie, N.C, Hayes R. D. and Trebits R. N., [Millimeter-Wave Radar Clutter], Artech House, Boston & London, 8-9 (1992)

[12] F. S. Marzano, S. Barbieri, G. Vulpiani and W. I. Rose, "Volcanic Ash Cloud Retrieval by Ground-Based Microwave Weather Radar, " IEEE Transactions on Geoscience and Remote Sensing, 44 (11), 3235-3246, (2006), doi: 10.1109/TGRS.2006.879116.

[13] Rogers, A.B, Macfarlane, D.G. and Robertson, D.A., "Complex Permittivity of Volcanic Rock and Ash at Millimeter Wave Frequencies," IEEE Geoscience and Remote Sensing Letters, 8 (2), 298-302 (2011), doi: 10.1109/LGRS.2010.2064756.

[14] Sauvageot, H., [Radar Meteorology], Artech House, Norwood, 88-91 (1992)

[15] Speirs, P.J., “Millimetre-wave radar measurement of rain and volcanic ash”, Thesis, University of St Andrews (2014)

[16] https://www.ecanechoicchambers.com/pdf/WAVASORB%20-%20VHP.pdf (17 March 2021)

Downloaded From: https://www.spiedigitallibrary.org/conference-proceedings-of-spie on 22 Apr 2021
Terms of Use: https://www.spiedigitallibrary.org/terms-of-use